Optimizing the balance between heterologous acetate- and CO2-reduction pathways in anaerobic cultures of Saccharomyces cerevisiae strains engineered for low-glycerol production

van Aalst, Aafke C.A.; Geraats, Ellen H.; Jansen, Mickel L.A.; Mans, Robert; Pronk, Jack T.

DOI
10.1093/femsyr/foad048

Publication date
2023

Document Version
Final published version

Published in
FEMS yeast research

FEMS Yeast Research, 2023, 23, 1–11
DOI: 10.1093/femsyr/foad048
Advance access publication date: 6 November 2023
Research Article

Optimizing the balance between heterologous acetate- and CO_2-reduction pathways in anaerobic cultures of *Saccharomyces cerevisiae* strains engineered for low-glycerol production

Aafke C.A. van Aalst [1], Ellen H. Geraats[1], Mickel L.A. Jansen[2], Robert Mans[1], Jack T. Pronk [1,*]

[1]Department of Biotechnology, Delft University of Technology, Van der Maasweg 9, 2629 HZ Delft , The Netherlands
[2]DSM Biotechnology Centre, Alexander Fleminglaan 1, 2613 AX Delft, The Netherlands
*Corresponding author. Department of Biotechnology, Delft University of Technology, Van der Maasweg 9, 2629 HZ Delft, The Netherlands. Tel: +31 15 2782416; E-mail: j.t.pronk@tudelft.nl
Editor: [Zengyi Shao]

Abstract

In anaerobic *Saccharomyces cerevisiae* cultures, NADH (reduced form of nicotinamide adenine dinucleotide)-cofactor balancing by glycerol formation constrains ethanol yields. Introduction of an acetate-to-ethanol reduction pathway based on heterologous acetylating acetaldehyde dehydrogenase (A-ALD) can replace glycerol formation as 'redox-sink' and improve ethanol yields in acetate-containing media. Acetate concentrations in feedstock for first-generation bioethanol production are, however, insufficient to completely replace glycerol formation. An alternative glycerol-reduction strategy bypasses the oxidative reaction in glycolysis by introducing phosphoribulokinase (PRK) and ribulose-1,5-bisphosphate carboxylase/oxygenase (RuBisCO). For optimal performance in industrial settings, yeast strains should ideally first fully convert acetate and, subsequently, continue low-glycerol fermentation via the PRK-RuBisCO pathway. However, anaerobic batch cultures of a strain carrying both pathways showed inferior acetate reduction relative to a strain expressing only the A-ALD pathway. Complete A-ALD-mediated acetate reduction by a dual-pathway strain, grown anaerobically on 50 g L^{-1} glucose and 5 mmol L^{-1} acetate, was achieved upon reducing PRK abundance by a C-terminal extension of its amino acid sequence. Yields of glycerol and ethanol on glucose were 55% lower and 6% higher, respectively, than those of a nonengineered reference strain. The negative impact of the PRK-RuBisCO pathway on acetate reduction was attributed to sensitivity of the reversible A-ALD reaction to intracellular acetaldehyde concentrations.

Keywords: acetate; biofuels; NADH; redox cofactor balance; fermentation

Background

Ethanol, predominantly produced by yeast-based fermentation of renewable carbohydrate feedstocks, can serve as a renewable automotive fuel and as precursor for a range of other products, including ethylene and jet fuel (Mohsenzadeh et al. 2017, Capaz et al. 2018). In industrial ethanol production, the sugar feedstock can account for up to 70% of the overall process costs (Pfromm et al. 2010). Maximizing the yield of ethanol on sugar is therefore of paramount importance for process economics. The current global fermentative production of ca. 100 M ton ethanol y^{-1} (Renewable Fuels Association: Annual Ethanol Production 2022) almost exclusively relies on the yeast *Saccharomyces cerevisiae*. Ethanol yields in yeast-based industrial processes can reach up to 92% of the theoretical maximum (Lopes et al. 2016), with a loss of substrate carbon primarily due to formation of yeast biomass and glycerol (Nissen et al. 2000).

In anaerobic cultures of wild-type *S. cerevisiae*, glycerol formation via the NAD^+-dependent glycerol-3-phosphate dehydrogenases Gpd1 and Gpd2 is essential for re-oxidation of 'surplus' NADH (reduced form of nicotaninamide adenine dinucleotide) formed in biosynthetic processes (Verduyn et al. 1990, Bakker et al. 2001). Multiple strategies have been explored to alter the metabolic network of *S. cerevisiae* to reduce NADH formation in biosynthetic reactions and/or rearrange yeast carbon metabolism to couple NADH re-oxidation to the formation of ethanol instead of glycerol (reviewed in van Aalst et al. 2022). Some of the latter engineering strategies can completely replace glycerol formation in anaerobic laboratory cultures. However, because of the importance of glycerol in yeast osmotolerance (Blomberg and Adler 1992), application-oriented engineering strategies typically aim at a strong reduction of glycerol formation rather than at its complete elimination (van Aalst et al. 2022).

Introduction of a heterologous acetylating acetaldehyde dehydrogenase (A-ALD) into *S. cerevisiae* enables the NADH-dependent reduction of acetyl-CoA to acetaldehyde, which can subsequently be reduced to ethanol by the native yeast alcohol dehydrogenase (Guadalupe-Medina et al. 2010). Coupling this reaction to heterologous pathways involving either phosphoketolase and phosphotransacetylase (Andrei and Munos 2017) or pyruvate–formate lyase (de Bont and Teunissen 2012, Argyros et al. 2015) can couple a net oxidation of NADH to the conversion of glucose to ethanol. In acetate-containing media, acetyl-CoA can alternatively be

Received 22 May 2023; **revised** 24 October 2023; **accepted** 3 November 2023

generated from acetate by yeast acetyl-CoA synthetase (ACS). *Saccharomyces cerevisiae* contains two ACS-encoding genes, *ACS1* and *ACS2*. Transcription of *ACS1* is repressed by glucose (Kratzer and Schüller 1995) and the Acs1 protein is subject to glucose catabolite inactivation (de Jong-Gubbels et al. 1997). In contrast, *ACS2* is functionally expressed in anaerobic, glucose-grown batch cultures (van den Berg et al. 1996). Acetic acid has a pK_a value of 4.76, so in cultures grown at pH 5, 37% of the total acetate content occurs in the undissociated form, which can diffuse over the yeast plasma membrane. Introduction of the *Escherichia coli* A-ALD EutE in *S. cerevisiae*, combined with deletion of *GPD2*, led to a 5-fold lower ratio between glycerol and biomass formation in anaerobic, acetate-supplemented cultures than in the nonengineered parental strain, without affecting specific growth rate (Papapetridis et al. 2017). However, the combined activity of native acetyl-CoA synthetase [Acs2, (van den Berg et al. 1996)], acetaldehyde dehydrogenases [Ald6, Ald5, and Ald4 (Saint-Prix et al. 2004)], and A-ALD can theoretically form an ATP-hydrolyzing reaction cycle (Papapetridis et al. 2016). Additional deletion of *ALD6* is therefore often applied in A-ALD-based redox-cofactor engineering strategies (Wei et al. 2013, Papapetridis et al. 2016, 2017).

Development of metabolic engineering strategies aimed at reduction of exogenous acetate to ethanol is predominantly inspired by industrial fermentation of lignocellulosic hydrolysates, in which acetate concentrations can exceed 5 g L^{-1} (Taherzadeh et al. 1997) and negatively affect yeast fermentation (Taherzadeh et al. 1997, Thomas et al. 2002).

In first-generation feedstocks, such as corn mash, acetate concentrations of up to 1.2 g L^{-1} are reported (Russell 2003, Rasmussen et al. 2015, Phibro Animal Health Corporation 2022), while glucose concentrations in industrial fermentation processes can reach 300 g L^{-1} (Kumar et al. 2020, Secches et al. 2022). During such fermentations, 12–15 g L^{-1} of glycerol is produced (Nissen et al. 2000, Kumar and Singh 2016). To replace the redox-cofactor-balancing role of this amount of glycerol, ~4 g L^{-1} of acetate would be required. First-generation feedstocks for ethanol production therefore typically do not contain enough acetate to replace all the glycerol produced.

Ideally, an engineered yeast strain for first-generation processes should reduce all available acetate to ethanol and, after acetate depletion, continue fast anaerobic growth with a low-glycerol yield by using another engineered, acetate-independent redox-balancing pathway. An engineered pathway meeting this description is based on bypassing the oxidative reaction in glycolysis by introducing the Calvin-cycle enzymes phosphoribulokinase (PRK) and ribulose-1,5-bisphosphate carboxylase/oxygenase (RuBisCO) (Guadalupe-Medina et al. 2013, Papapetridis et al. 2018). Performance of this pathway as a redox-cofactor balancing pathway in yeast was improved by overexpression of structural genes for enzymes of the nonoxidative pentose-phosphate pathway (non-ox PPP↑; p*TDH3-RPE1*, p*PGK1-TKL1*, p*TEF1-TAL1*, p*PGI1-NQM1*, p*TPI1-RKI1*, and p*PYK1-TKL2*) and deletion of *GPD2* (Papapetridis et al. 2018). In addition, multiple copies of an expression cassette for bacterial *cbbM* RuBisCO were integrated in the yeast genome to improve conversion of ribulose-5-bisphosphate into 3-phosphoglycerate (Papapetridis et al. 2018). While, initially, up to 15 copies of the *cbbM* cassette were integrated (Papapetridis et al. 2018), a later study indicated that two copies were sufficient (van Aalst et al. 2023). Expression of a spinach *PRK* gene from the anaerobically inducible *DAN1* promoter limited toxic effects of PRK during aerobic precultivation (Papapetridis et al. 2018). The resulting PRK-RuBisCO-synthesizing *S. cerevisiae* strain (IMX2736; Δ*gpd2*, non-ox PPP↑, p*DAN1-PRK*, 2x *cbbM*, *GroES/GroEL*) showed essentially the same maximum growth rate on glucose as a nonengineered reference strain in anaerobic batch bioreactors while exhibiting a 96% lower glycerol yield and a 10% higher ethanol yield on glucose than the reference strain (van Aalst et al. 2023).

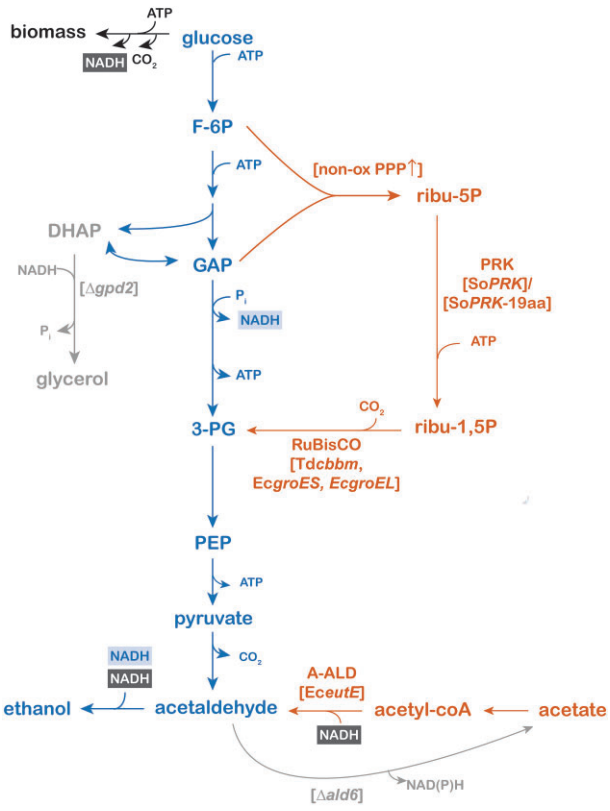

Figure 1. Schematic representation of ethanol and biomass formation from glucose and acetate by an engineered strain of *S. cerevisiae* that expresses heterologous genes encoding the enzymes PRK, RuBisCO, and A-ALD. Genetic modifications are indicated between square brackets. Blue: native reactions of the redox-neutral conversion of glucose to ethanol via glycolysis and alcoholic fermentation. Black: biosynthetic reactions with a net input of ATP and a net production of CO_2 and NADH. Orange: heterologous reduction pathways for NADH recycling either via a nonoxidative bypass of glycolysis via PRK-RuBisCO or via acetyl-coA reduction via A-ALD using exogenous acetate. Grey: native pathways, which are (partially) impaired by deletion of a key gene. Heterologous genes encode the following enzymes: Ec*eutE*, *E. coli* A-ALD; So*PRK*, *S. oleracea* PRK; Td*cbbM*, *T. denitrificans* RuBisCO; and Ec*groEL* and Ec*groES*, *E. coli* GroEL and GroES, respectively. Abbreviations indicate the following metabolites: F-6P, fructose-6-phosphate; GAP, glyceraldehyde-3-phosphate; DHAP, dihydroxyacetone phosphate, 3-PG, 3-phosphoglycerate; PEP, phosphoenolpyruvate; ribu-5P, ribulose-5-phosphate; and ribu-1,5P, ribulose-1,5-bisphosphate. 19aa indicates a 19 amino acid C-terminal extension sequence (van Aalst et al. 2023).

The A-ALD and PRK-RuBisCO-based strategies have both been shown to re-oxidize surplus NADH in anaerobic yeast cultures (Papapetridis et al. 2017, 2018) and, in particular, in Δ*gpd2* genetic backgrounds, to efficiently compete for NADH with the native glycerol pathway. However, interaction of these two strategies upon their implementation of a single yeast strain has not yet been investigated. The goal of the present study is therefore to study growth and product formation in acetate-containing media of dual-pathway *S. cerevisiae* strains that express both the A-ALD pathway and the PRK-RuBisCO pathway (Fig. 1). To this end, engineered strains were grown in anaerobic bioreactor cultures on glucose, using media in which acetate concentrations were

either sufficient or insufficient to complete re-oxidation of surplus NADH by acetate reduction. Based on observed patterns of growth and (by)product formation, further engineering was aimed at improving acetate reduction via A-ALD in PRK-RuBisCO-expressing strains.

Materials and methods

Growth media and strain maintenance

Saccharomyces cerevisiae strains constructed and/or used in this study (Table 1) all originate from the CEN.PK lineage (Entian and Kötter 2007, Nijkamp et al. 2012). Yeast strains were propagated in yeast extract peptone dextrose medium [YPD; 10 g L^{-1} Bacto yeast extract (Thermo Fisher Scientific, Waltham, MA), 20 g L^{-1} Bacto™ peptone (Thermo Fisher Scientific), 20 g L^{-1} glucose] or synthetic medium with vitamins [SM; 3.0 g L^{-1} KH_2PO_4, 0.5 g L^{-1} $MgSO_4{\cdot}7H_2O$, 5.0 g L^{-1} $(NH_4)_2SO_4$, (Verduyn et al. 1992)] prepared and sterilized as described previously. Concentrated solutions of glucose were autoclaved separately for 20 min at 110°C and supplemented to SM to a final concentration of 20 or 50 g L^{-1}. For growth of uracil-auxotrophic strains, 150 mg L^{-1} uracil was added to SM by adding a concentrated uracil solution (3.75 g L^{-1}) autoclaved at 120°C for 20 min (Pronk 2002). To select for presence of an acetamidase marker cassette (Solis-Escalante et al. 2013), $(NH_4)_2SO_4$ was replaced by 6.6 g L^{-1} K_2SO_4 and 0.6 g L^{-1} filter-sterilized acetamide. Where indicated, acetic acid (≥99.8%, Honeywell, Charlotte, NC) was added to media to a concentration of 0.3 or 3 g L^{-1}. A concentrated stock solution of Tween 80 (polyethylene glycol sorbitan monoelate; Merck, Darmstadt, Germany) and ergosterol (98%; Acros Organics-Thermo Fisher Scientific) (420 g L^{-1} Tween and 10 g L^{-1} ergosterol) was prepared in absolute ethanol (Supelco: Sigma–Aldrich, St. Louis, MI). For anaerobic cultivation, 1 mL of this solution was added per litre of medium (Mooiman et al. 2021). *Escherichia coli* XL1-Blue stock cultures were propagated in lysogeny broth (LB) medium (Bertani 2004). For strain maintenance, glycerol (30% v/v final concentration) was added to late exponential phase cultures and stored at −80°C. Solid media were prepared by adding 20 g L^{-1} Bacto agar (Becton Dickinson, Breda, The Netherlands) to mineral salts solutions. Vitamin solution, glucose and, when required, acetamide were added to SM-agar media after cooling to 60°C. *Saccharomyces cerevisiae* cultures on agar plates were incubated at 30°C until colonies appeared (1–5 days) and *E. coli* cultures on plates were incubated overnight at 37°C.

Construction of plasmids and expression cassettes

DNA fragments for construction of plasmids and expression cassettes were PCR amplified with Phusion High Fidelity DNA Polymerase (Thermo Fisher Scientific) according to the manufacturer's manual. Diagnostic colony PCR was performed using DreamTaq polymerase (Thermo Fisher Scientific). DNA fragments were separated by electrophoresis on 1% (w/v) agarose (Sigma–Aldrich) gels in 1xTAE (40 mM Tris-acetate pH 8.0 and 1 mM EDTA). Fragments were isolated from gels with the Zymoclean Gel DNA Recovery kit (Zymo Research, Irvine, CA) or isolated from PCR mixes with a GeneJET kit (Thermo Fisher Scientific). DNA concentrations were measured with a NanoDrop 2000 spectrophotometer (wavelength 260 nm; Thermo Fisher Scientific). Plasmid assembly was performed by *in-vitro* Gibson assembly using a HiFi DNA Assembly Master Mix (New England Biolabs, Ipswich, MA), downscaled to 5 μL reaction volume. One microlitre of reaction mixture was used for heat-shock transformation (Froger and Hall 2007) of *E. coli* XL-1 Blue. Plasmids were isolated from *E. coli* XL-I Blue transformants with the Sigma GenElute Plasmid Kit (Sigma–Aldrich) according to the manufacturer's instructions. Plasmids used and constructed in this study are listed in Table 2 and oligonucleotide primers are listed in Supplementary Table S1.

A unique Cas9-recognition sequence in *GPD2* was identified as described previously (Mans et al. 2015). pUDR744 was constructed by PCR amplification of pROS10 with primer 5793 to obtain a linear backbone, and PCR amplification of pROS10 with primer 7839 to obtain the insert fragment containing the *GPD2* gRNA. The plasmid was then assembled by *in-vitro* Gibson Assembly. A p*TDH3-eutE*-tCYC1 integration cassette was obtained by PCR amplification with primers 16 615/16 616 with pUDI076 as template, adding 60 bp terminal sequences homologous to sequences directly upstream and downstream of the coding region of *ALD6*. A dsDNA repair fragment for *GDP2* deletion was obtained by mixing primers 6969/6970 in a 1:1 molar ratio, heating the mixture to 95°C for 5 min and subsequently cooling down at room temperature.

Yeast genome editing

The lithium−acetate method (Gietz and Woods 2001) was used for yeast transformation. Correct Cas9-mediated integration or deletion was routinely verified by diagnostic PCR and single-colony isolates were restreaked thrice on SMD (SM with 20 g L^{-1} glucose) and stored at −80°C.

Saccharomyces cerevisiae IMX2302 was constructed by co-transforming strain IMX2288 with pUDR264 and repair fragment p*TDH3-eutE*-tCYC1 (with homologous flanks to the upstream and downstream sequence of *ALD6* open reading frame). Transformants were selected on SMD with acetamide and uracil. To restore uracil prototrophy, strain IMX2302 was transformed with the *URA3*-carrying plasmid p426-*TEF* (empty vector), yielding strain IMX2502.

Strain IMX2503 was constructed by co-transforming IMX581 with gRNA-plasmids pUDR744 (targeting *GPD2*) and pUDR264 (targeting *ALD6*) and repair fragments for *GPD2* deletion (dsDNA homologous to the upstream and downstream sequence of *GPD2* open reading frame) and p*TDH3-eutE*-tCYC1 (with homologous flanks to the upstream and downstream sequence of *ALD6* open reading frame). Transformants were selected on SMD with acetamide. pUDR264 was removed by selection on SMD, while pUDR744 was retained to support uracil prototrophy.

Strain IMX2723 was obtained from IMX2593 by co-transforming with gRNA-plasmid pUDR264 and repair fragment p*TDH3-eutE*-tCYC1. Transformants were selected on SMD with acetamide. pUDR264 was removed by selection on SMD, while pUDR103 was retained to support uracil prototrophy.

Aerobic shake-flask cultivation

Shake-flask cultures were grown at 30°C in 500-mL round-bottom shake-flasks containing 100 mL medium, placed in an Innova incubator shaker (Eppendorf Nederland B.V., Nijmegen, The Netherlands) and shaken at 200 rpm.

Bioreactor cultivation

Anaerobic bioreactor batch cultivation was conducted at 30°C in 2-L bioreactors (Applikon Getinge, Delft, The Netherlands), with a working volume of 1 L. Culture pH was kept constant at 5.0 by automatic addition of 2 M KOH. All bioreactor cultures were grown on synthetic medium supplemented with vitamins, glucose, acetic acid, the anaerobic growth factors Tween 80 (420 mg

Table 1. *Saccharomyces cerevisiae* strains used in this study.

Strain name	Relevant genotype	Parental strain	Origin
CEN.PK113-5D	*MATa ura3-52*		Entian and Kötter (2007)
IMX581	*MATa ura3-52 can1::cas9-natNT2*	CEN.PK113-5D	Mans et al. (2015)
IME324	*MATa ura3-52 can1::cas9-natNT2* p426-TEF (*URA3*)	IMX581	Papapetridis et al. (2018)
IMX2288	*MATa ura3-52 can1::cas9 natNT2 gpd2::*(p*TDH3-RPE1*, p*PGK1-TKL1*, p*TEF1-TAL1*, p*PGI1-NQM1*, p*TPI1-RKI1*, p*PYK1-TKL2*) *sga1::*(p*DAN1-PRK*, *cbbM (2 copies) groEL, groES*)		van Aalst et al. (2023)
IMX2302	*MATa ura3-52 can1::cas9 natNT2 gpd2::*(p*TDH3-RPE1*, p*PGK1-TKL1*, p*TEF1-TAL1*, p*PGI1-NQM1*, p*TPI1-RKI1*, p*PYK1-TKL2*) *sga1::*(p*DAN1-PRK*, *cbbM (2 copies) groEL, groES*) *ald6::eutE*	IMX2288	This study
IMX2502	*MATa ura3-52 can1::cas9 natNT2 gpd2::*(p*TDH3-RPE1*, p*PGK1-TKL1*, p*TEF1-TAL1*, p*PGI1-NQM1*, p*TPI1-RKI1*, p*PYK1-TKL2*) *sga1::*(p*DAN1-PRK*, *cbbM (2 copies) groEL, groES*) *ald6::eutE* p426-*TEF* (*URA3*)	IMX2302	This study
IMX2503	*MATa ura3-52 can1::cas9 natNT2 ald6::eutE*, Δ *gpd2* pUDR774 (*KlURA3*)	IMX581	This study
IMX2593	*MATa ura3-52 can1::cas9-natNT2 gpd2::*(p*TDH3-RPE1*, p*PGK1-TKL1*, p*TEF1-TAL1*, p*PGI1-NQM1*, p*TPI1-RKI1*, p*PYK1-TKL2*) *sga1::*(p*DAN1-PRK*-19aa, *cbbM (2 copies) groEL, groES*) pUDR103 (*KlURA3*)		van Aalst et al. (2023)
IMX2723	*MATa ura3-52 can1::cas9-natNT2 gpd2::*(p*TDH3-RPE1*, p*PGK1-TKL1*, p*TEF1-TAL1*, p*PGI1-NQM1*, p*TPI1-RKI1*, p*PYK1-TKL2*) *sga1::*(p*DAN1-PRK*-19aa, *cbbM (2 copies) groEL, groES*) *ald6::eutE* pUDR103 (*KlURA3*)	IMX2593	This study

Kl denotes *Kluyveromyces lactis*.

Table 2. Plasmids used in this study. Kl denotes Kluyveromyces lactis

Plasmid name	Characteristics	Reference
p426_TEF	2 μm ori, *URA3*, p*TEF1*-t*CYC1* (empty vector)	Mumberg et al. (1995)
pMEL10	2 μm ori, *KlURA*, gRNA-*CAN1.Y*	Mans et al. (2015)
pMEL11	2 μm ori, *AmdS*, gRNA-*CAN1.Y*	Mans et al. (2015)
pROS10	2 μm ori, *KlURA3*, gRNA-*CAN1.Y* gRNA-*ADE2.Y*	Mans et al. (2015)
pUDI076	pRS406-*TDH3*p-*eutE*-*CYC1*t	Papapetridis et al. (2016)
pUDR103	2 μm ori, *KlURA3*, gRNA-*SGA1.Y*	Papapetridis et al. (2018)
pUDR264	2 μm ori, *AmdS*, gRNA.*ALD6.Y*	Papapetridis et al. (2016)
pUDR744	2 μm ori, *KlURA3*, gRNA.*GPD2.Y* gRNA.*GPD2.Y*	This work

Kl denotes *Kluyveromyces lactis*.

L^{-1}) and ergosterol (10 mg L^{-1}), and 0.2 g L^{-1} antifoam C (Sigma–Aldrich). Cultures were sparged at 0.5 L min^{-1} with an N_2/CO_2 (90/10%) gas mixture. The outlet gas stream was cooled to 4°C in a condenser to minimize evaporation. Oxygen diffusion was minimized by use of Norprene tubing (Saint-Gobain, Amsterdam, The Netherlands) and Viton O-rings (ERIKS, Haarlem, The Netherlands). Inocula were prepared in 500-mL shake flasks containing 100 mL SMD. A first starter culture was inoculated with a frozen stock culture, grown aerobically for 15–18 h at 30°C and used to inoculate precultures on SMD. Upon reaching midexponential phase (OD_{660} of 3–5), these were used to inoculate bioreactor cultures at an initial OD_{660} of 0.25–0.40.

Analytical methods

Growth was monitored by biomass dry weight measurements (Guadalupe-Medina et al. 2013) and by measuring optical density at 660 nm (OD_{660}) on a Jenway 7200 spectrophotometer. Metabolite concentrations were determined by high-performance liquid chromatography (Guadalupe-Medina et al. 2013). A first-order evaporation rate constant of 0.008 h^{-1} was used to correct ethanol concentrations for evaporation (Guadalupe-Medina et al. 2013). Acetaldehyde concentrations were determined in the off-gas and the broth by derivatization using 2,4-DNPH as described previously (van Aalst et al. 2023). As carbon recoveries could not be accurately calculated due to the high concentration of CO_2 in the inlet gas of bioreactor cultures, electron recoveries based on degree of reduction of relevant compounds (Roels 1980) were used instead.

Yields and stoichiometries calculations

In batch cultures on 20 g L^{-1} of glucose and 50 mmol L^{-1} of acetate, product yields on glucose were calculated using concentration measurements on at least six samples taken during the exponential growth phase. Yields were then determined from the slopes of the resulting linear fits. In batch cultures grown on 50 g L^{-1} of glucose and 5 mmol L^{-1} of acetate, growth-rate dynamics implied that stoichiometries of glucose and products could not *a priori* be assumed to be constant over time. Yields of products were therefore first calculated based on concentrations at the first two sampling points and the two final sampling points of each batch fermentation experiments. Ethanol yields for these cultures were additionally estimated from linear fits of consumed glucose versus produced ethanol (Supplementary Fig. S4). Acetate consumption per mole of glucose was calculated from measurements taken before acetate depletion.

Data representation

All quantitative growth studies were performed in duplicate experiments performed in different bioreactors. Biomass-specific

Table 3. Specific growth rate, stoichiometries of biomass and (by)product formation and biomass-specific acetate consumption rates in anaerobic bioreactor batch cultures of *S. cerevisiae* strains IME324 (reference strain), IMX2503 (Δ*gpd2* Δ*ald6* p*TDH3-eutE*), and IMX2502 (non-ox PPP↑ Δ*gpd2* Δ*ald6* p*TDH3-eutE* p*DAN1-PRK* 2x p*TDH3-cbbM* p*TPI1-groES pTEF1-groEL*).

Strain Relevant genotype	IME324 Reference	IMX2503 *gpd2Δ ald6Δ eutE*	IMX2502 *gpd2Δ ald6Δ eutE PRK 2x cbbM*
μ (h^{-1})	0.31 ± 0.00	0.32 ± 0.00	0.25 ± 0.01
$Y_{biomass/glucose}$ (g_x g^{-1})	0.071 ± 0.003	0.081 ± 0.001	0.072 ± 0.001
$Y_{ethanol/glucose}$ (mol mol^{-1})	1.65 ± 0.02	1.76 ± 0.01	1.71 ± 0.00
$Y_{acetaldehyde/glucose}$ (mol mol^{-1})	<0.005	<0.005	0.026 ± 0.001
$Y_{glycerol/glucose}$ (mol mol^{-1})	0.117 ± 0.000	0.033 ± 0.000	0.024 ± 0.002
$Y_{acetate/glucose}$ (mol mol^{-1})	−0.032 ± 0.004	−0.084 ± 0.002	−0.023 ± 0.001
Glycerol production (mmol g_x^{-1})	8.5 ± 0.1	2.1 ± 0.1	1.8 ± 0.1
Acetate consumption (mmol g_x^{-1})	2.3 ± 0.3	5.7 ± 0.3	1.7 ± 0.1
$q_{acetate}$ (mmol g_x^{-1} h^{-1})	−0.7 ± 0.0	−1.8 ± 0.1	−0.4 ± 0.0
Electron recoveries (%)	99–101	99–100	100–101

Cultures were grown on synthetic medium with 20 g L^{-1} of glucose and 50 mmol L^{-1} of acetate at pH 5 and at 30°C and sparged with a 90:10 mixture of N_2 and CO_2. Stoichiometries of biomass and metabolite production formation were calculated from at least six sampling points in the exponential growth phase. Values represent averages ± mean deviations of measurements on independent duplicate cultures. Since the high concentration of CO_2 in the inlet gas precluded construction of carbon balances, degree-of-reduction balances were used to verify data consistency (Roels 1980). Non-ox PPP↑ indicates the integration of the expression cassettes of p*TDH3-RPE1*, p*PGK1-TKL1*, p*TEF1-TAL1*, p*PGI1-NQM1*, p*TPI1-RKI1*, and p*PYK1-TKL2*. Symbols: μ, specific growth rate; g_x, gram biomass; *Y*, yield; $q_{acetate}$: biomass-specific rate of acetate consumption in exponential growth phase.

Table 4. Stoichiometries of biomass and (by)product formation and biomass, ethanol, glycerol, and acetate yield on glucose of anaerobic bioreactor batch cultures of *S. cerevisiae* strains IME324 (reference strain), IMX2503 (Δ*gpd2* Δ*ald6* p*TDH3-eutE*), IMX2502 (non-ox PPP↑ Δ*gpd2* Δ*ald6* p*TDH3-eutE* p*DAN1-PRK* 2x p*TDH3-cbbM* p*TPI1-groES pTEF1-groEL*), and IMX2723 (non-ox PPP↑ Δ*gpd2* Δ*ald6* p*TDH3-eutE* p*DAN1-PRK*-19aa 2x p*TDH3-cbbM* p*TPI1-groES pTEF1-groEL*).

Strain Relevant genotype	IME324 Reference	IMX2503 Δ*gpd2* Δ*ald6 eutE*	IMX2502 Δ*gpd2* Δ*ald6 eutE PRK 2x cbbM*	IMX2723 Δ*gpd2* Δ*ald6 eutE* PRK-19aa (van Aalst et al. 2023) 2x *cbbM*
$Y_{biomass/glucose}$ (g_x g^{-1})	0.084 ± 0.000	0.083 ± 0.000	0.073 ± 0.001	0.087 ± 0.001
$Y_{ethanol/glucose}$ (mol mol^{-1})	1.55 ± 0.01	1.58 ± 0.00	1.59 ± 0.01	1.64 ± 0.01
$Y_{glycerol/glucose}$ (mol mol^{-1})	0.150 ± 0.000	0.125 ± 0.000	0.053 ± 0.000	0.070 ± 0.002
$Y_{acetate/glucose}$ (mol mol^{-1})	-0.004 ± 0.000	-0.067 ± 0.002	-0.021 ± 0.002	-0.053 ± 0.009
Glycerol production (mmol g_x^{-1})	9.9 ± 0.0	8.2 ± 0.0	4.3 ± 0.1	4.5 ± 0.1
Acetate consumption (mmol g_x^{-1})	0.2 ± 0.0	3.5 ± 0.2	1.4 ± 0.2	2.5 ± 0.0
Electron recovery	99–99	99–99	94–94	99–99

Cultures were grown on synthetic medium with 50 g L^{-1} of glucose and 5.0 mmol L^{-1} acetate at pH 5 and at 30°C and sparged with a 90:10 mixture of N_2 and CO_2. Since the high concentration of CO_2 in the inlet gas precluded construction of accurate carbon balances, degree-of-reduction balances were used to verify data consistency (Roels 1980). Non-ox PPP↑ indicates the integration of the expression cassettes of p*TDH3-RPE1*, p*PGK1-TKL1*, p*TEF1-TAL1*, p*PGI1-NQM1*, p*TPI1-RKI1* and p*PYK1-TKL2*. Symbols: x, biomass; *Y*, yield. Values represent averages ± mean deviations of measurements on independent duplicate cultures.

rates and yields calculated from duplicate experiments are generally highly reproducible (as indicated by the standard errors included in Tables 3 and 4). However, during inoculation by transfer of independent replicate shake-flask precultures into bioreactors, slight offsets can occur in the growth curves. Especially during the exponential growth phase, small offsets can result in quite large differences in metabolite concentrations. As a consequence, combination of data from replicate cultures in a single figure, with averages and error bars can lead to 'messy', difficult to interpret figures. Therefore, figures show data from single growth experiments, while the replicates are shown in Supplementary Materials, along with relevant primary data.

Whole-genome sequencing

Genomic DNA was isolated from an aerobic shake-flask culture (100 mL) on SMD of *S. cerevisiae* strain IMX2503, at late-exponential-phase (OD_{660} of 10–15), using a Qiagen Blood & Cell Culture DNA kit and 100/G Genomics-tips (Qiagen, Hilden, Germany). Short-read paired-end whole-genome sequencing was performed commercially on a 350-bp PCR-free insert library using Illumina SBS technology (Macrogen, Amsterdam, The Netherlands). Sequence reads were mapped against the genome of *S. cerevisiae* CEN.PK113-7D (Salazar et al. 2017) to which a virtual contig containing p*TDH3-eutE* had been added, and processed as described previously (van Aalst et al. 2022).

Results

Suboptimal acetate conversion by a yeast strain harbouring both an A-ALD-dependent acetate-reduction and PRK-RuBisCO pathway

Saccharomyces cerevisiae Δ*gpd2* strains expressing a bacterial A-ALD gene can use exogenous acetate as electron acceptor for anaerobic re-oxidation of 'surplus' NADH generated in biosynthesis (Verduyn et al. 1990). Consistent with earlier reports (Papapetridis et al. 2017), *S. cerevisiae* IMX2503 (Δ*ald6* Δ*gpd2 eutE*)

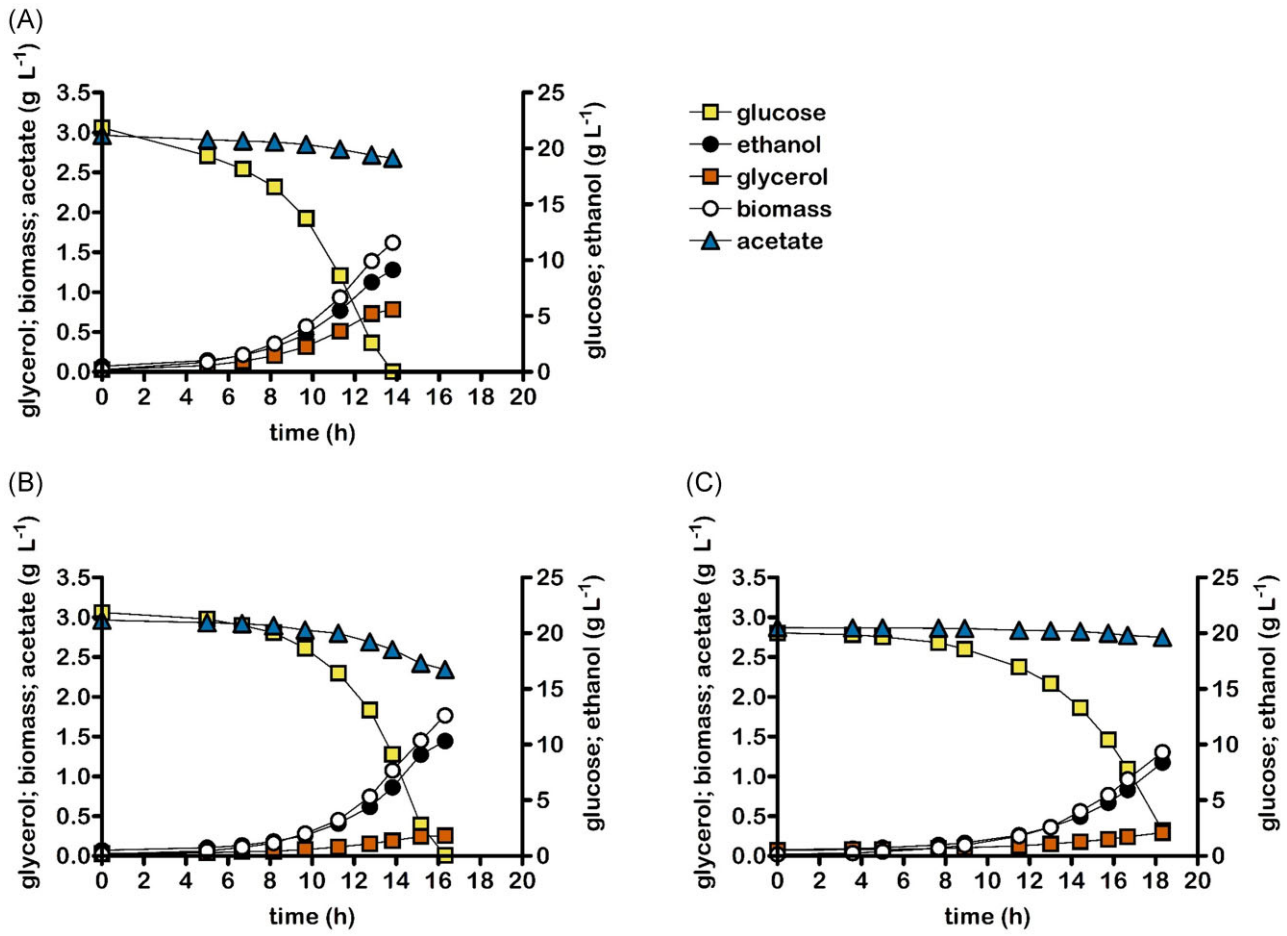

Figure 2. Concentrations of biomass, ethanol, glycerol, and acetate in anaerobic bioreactor batch cultures of *S. cerevisiae* strains IME324 (reference strain, A), IMX2503 (Δ*gpd2* Δ*ald6* p*TDH3-eutE*, B), and IMX2502 (non-ox PPP↑ Δ*gpd2* Δ*ald6* p*TDH3-eutE* p*DAN1-PRK* 2x p*TDH3-cbbM* p*TPI1-groES* p*TEF1-groEL*, C). cultures were grown anaerobically at pH 5.0 and at 30°C on synthetic medium containing 20 g L^{-1} glucose and 50 mmol L^{-1} acetate. Non-ox PPP↑ indicates the integration of the expression cassettes of p*TDH3-RPE1*, p*PGK1-TKL1*, p*TEF1-TAL1*, p*PGI1-NQM1*, p*TPI1-RKI1*, and p*PYK1-TKL2*. Representative cultures of independent duplicate experiments are shown, corresponding replicate of each culture shown in Additional file 3: Supplementary Fig. S2.

produced 76% less glycerol per amount of biomass formed than the reference strain IME324 (*ALD6 GPD2*) when grown in anaerobic bioreactor batch cultures on 20 g L^{-1} of glucose and 50 mmol L^{-1} acetate (Table 3, Fig. 2A and B). This acetate concentration was ∼5-fold higher than what was calculated to be required for complete re-oxidation of surplus NADH via A-ALD-mediated acetate reduction (Guadalupe-Medina et al. 2010, van Aalst et al. 2022). Specific growth rates of the two strains were not significantly different, but strain IMX2503 showed a 6.7% higher ethanol yield on glucose than the reference strain. Slow, EutE-independent consumption of acetate by anaerobic, glucose-grown batch cultures of nonengineered *S. cerevisiae* (Table 3, Fig. 2A) was previously shown to cease upon glucose depletion (Guadalupe-Medina et al. 2010) and attributed to the use of acetate-derived acetyl-CoA as a biosynthetic precursor (Flikweert et al. 1999).

Saccharomyces cerevisiae IMX2502 (Δ*gpd2* Δ*ald6 eutE* non-ox PPP↑ *PRK* 2x *cbbM groES/groEL*) combined the genetic modifications in the acetate-reducing strain IMX2503 with introduction of a nonoxidative bypass of glycolysis via PRK and RuBisCO (CbbM) (van Aalst et al. 2023). Under the conditions described above, this strain showed an even lower rate of acetate consumption than the reference strain IME324 (Table 3, Fig. 2C). Apparently, simultaneous presence of the two engineered pathways prevented efficient acetate reduction via EutE. However, strain IMX2502 produced 79% less glycerol per amount of biomass than the reference strain IME324, indicating that the PRK-RuBisCO bypass actively contributed to re-oxidation of surplus NADH.

Despite its low-glycerol formation, strain IMX2502 displayed a mere 4% higher ethanol yield than the reference strain IME324 and a slightly lower ethanol yield than the acetate-reducing strain IMX2503 (Table 3). This increase is ∼55% lower than theoretically predicted (van Aalst et al. 2022) and reported (van Aalst et al. 2023) for anaerobic glucose-grown cultures of a congenic 'PRK-RuBisCO-only' strain. This lower-than-anticipated ethanol yield of strain IMX2502 coincided with production of up to 2.7 ± 0.1 mmol L^{-1} acetaldehyde, a by-product that was not detected in cultures of the acetate-reducing strain IMX2503 and the reference strain IME324 (Table 3). Formation of acetaldehyde and acetate by slow-growing cultures of PRK-RuBisCO-based *S. cerevisiae* strains was previously attributed to an *in-vivo* overcapacity of the nonoxidative bypass of glycolysis (van Aalst et al. 2023). The acetaldehyde yield on glucose of strain IMX2502 was 3.6-fold higher than previously reported for anaerobic glucose-grown batch cultures of a congenic PRK-RuBisCO-strain [0.007 ± 0.001 mol acetaldehyde (mol glucose)$^{-1}$ (van Aalst et al. 2023)].

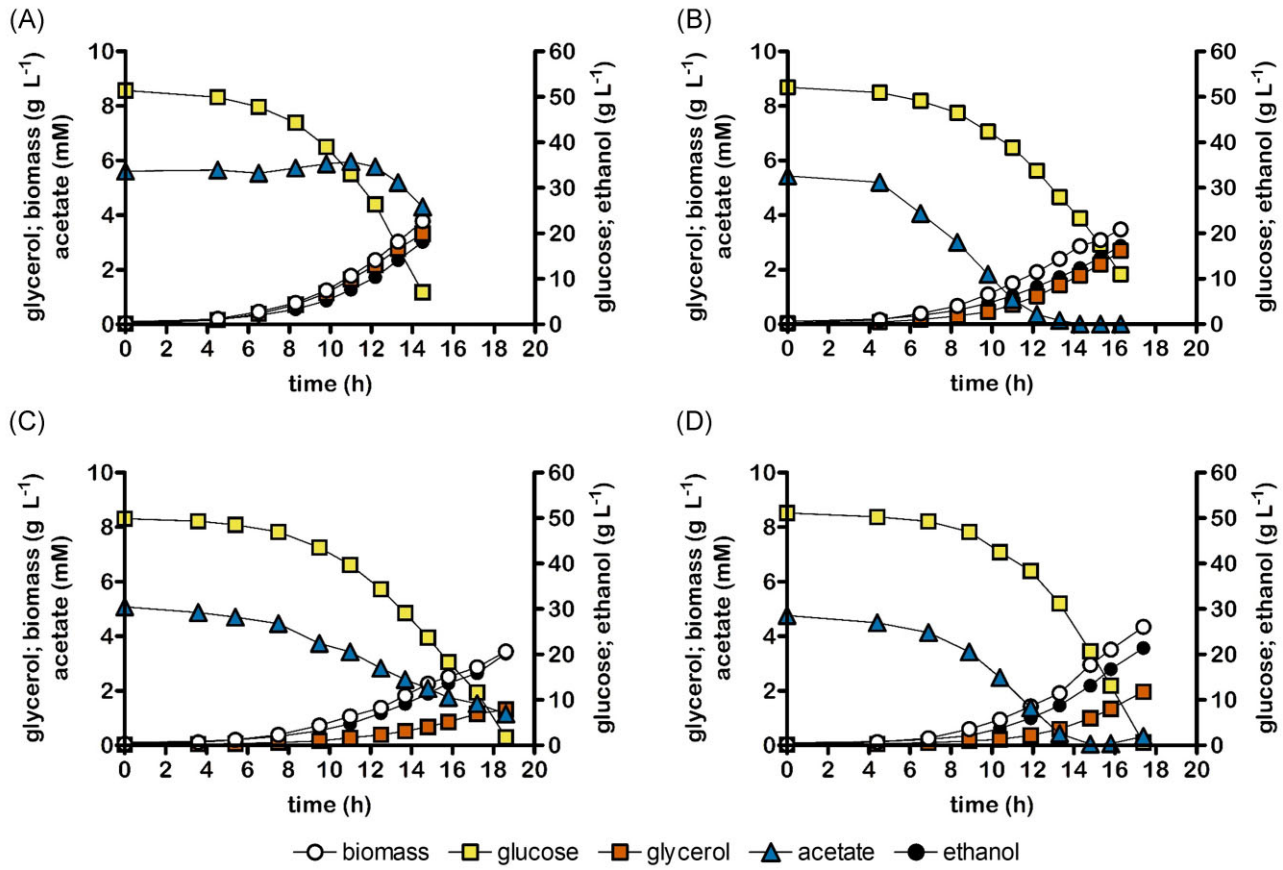

Figure 3. Concentrations of biomass, ethanol, glycerol, and acetate in anaerobic bioreactor batch cultures of *S. cerevisiae* strains IME324 (reference strain, A), IMX2503 (Δ*gpd2* Δ*ald6* p*TDH3-eutE*, B), IMX2502 (non-ox PPP↑ Δ*gpd2* Δ*ald6* p*TDH3-eutE* p*DAN1-PRK* 2x p*TDH3-cbbM* p*TPI1-groES* p*TEF1-groEL*, C), and IMX2723 [non-ox PPP↑ Δ*gpd2* Δ*ald6* p*TDH3-eutE* p*DAN1-PRK*-19aa (van Aalst et al. 2023) 2x p*TDH3-cbbM* p*TPI1-groES* p*TEF1-groEL*, D]. Cultures were grown anaerobically at pH 5.0 and at 30°C on synthetic medium containing 50 g L^{-1} glucose and 5.0 mmol L^{-1} acetate. Non-ox PPP↑ indicates the integration of the expression cassettes of p*TDH3-RPE1*, p*PGK1-TKL1*, p*TEF1-TAL1*, p*PGI1-NQM1*, p*TPI1-RKI1*, and p*PYK1-TKL2*. Representative cultures of independent duplicate experiments are shown, corresponding replicate of each culture shown in Additional file 3: Fig. S3.

Performance of engineered strains at low acetate-to-glucose ratios

To explore performance of engineered strains at acetate-to-glucose ratios that are more representative for those in first-generation feedstocks such as corn mash, anaerobic bioreactor batch cultures were grown on 50 g L^{-1} of glucose and 5 mmol L^{-1} acetate (Fig. 3, Table 4). Biomass and ethanol yields on glucose of the reference strain IME324 in these cultures were 32% higher and 10% lower, respectively, than in cultures grown at the higher acetate-to-glucose ratio (Tables 3 and 4). These results are in line with a higher maintenance-energy requirement in cultures grown at 50 mmol L^{-1} acetate, caused by weak-acid uncoupling of the plasma-membrane pH gradient (Narendranath et al. 2001).

Expressed per amount of formed biomass, acetate consumption by strain IME324 was ca. 10-fold lower than in cultures grown at the higher acetate-to-glucose ratio (Tables 3 and 4, respectively) and about two-thirds of the added 5 mmol L^{-1} acetate was expected to remain unused upon glucose depletion based on the consumption stoichiometry observed throughout the experiment (Fig. 3). In contrast, cultures of strain IMX2503 (Δ*ald6* Δ*gpd2 eutE*) completely consumed acetate under these conditions (Fig. 3). However, strain IMX2503 showed a mere 12% lower overall glycerol production per amount of biomass formed than the reference strain IME324 (Table 4), as compared to a 76% lower value in cultures grown at a high acetate-to-glucose ratio (Table 3).

Consistent with the small difference in glycerol yield, ethanol yields on glucose of the two strains measured in cultures grown at the low acetate-to-glucose ratio were not significantly different. These results are consistent with the dynamics of acetate consumption in the low-acetate cultures of strain IMX2503, which showed a progressive decrease of the biomass-specific rate of acetate consumption during the first phase of batch cultivation (Additional file 3, Supplementary Fig. S1). This may reflect the high K_m (ca. 8.8 mM) of Acs2, the sole acetyl-coenzyme A synthetase isozyme expressed in anaerobic batch cultures of *S. cerevisiae* (van den Berg et al. 1996). The decreasing biomass-specific rate of acetate conversion of strain IMX2503 forced a progressively larger fraction of surplus NADH to be reoxidized via Gpd1-dependent glycerol formation. When, after only approximately half of the glucose had been consumed, acetate was depleted (Fig. 3), this requirement became absolute and, as in wild-type *S. cerevisiae* (Nissen et al. 2000), further anaerobic growth became strictly coupled to glycerol production.

In cultures of the dual-pathway-strain IMX2502 (Δ*gpd2* Δ*ald6 eutE* non-ox PPP↑ *PRK* 2x *cbbM groES/groEL*) grown at a low acetate-to-glucose ratio, glycerol production per amount of biomass was 65% and 49% lower, respectively, than in corresponding cultures of the reference strain IME324 and the acetate-reducing strain IMX2503 (Table 4). However, acetate consumption expressed per amount of biomass formed by strain IMX2502 was 2.6-fold lower

than in cultures of strain IMX2503 (Table 4) and, upon glucose depletion, not all acetate had been consumed (Fig. 3). A 6% to 7% gap in the degree-of-reduction balance for low-acetate cultures of the dual-pathway-strain IMX2502 (Table 4) probably suggested that, as observed for cultures of this strain grown at a high acetate-to-glucose ratio (Table 3), acetaldehyde was formed as a byproduct. This interpretation was also consistent with an only slightly (2%) higher ethanol yield on glucose and a 14% lower biomass yield relative than observed for the reference strain IME324 (Table 4).

Despite the dynamics of the batch cultures shown in Fig. 3, glucose consumption and ethanol production by all four strains showed near-perfect linear fits over the entire duration of the experiments, indicating a near-constant ethanol yield for each strain (Supplementary Fig. S4). Ethanol yields calculated from these linear fits were essentially the same as those calculated from initial and final sample points (Supplementary Fig. S4, Table 4).

Tuning the PRK-RuBisCO pathway for improved acetate conversion in an A-ALD-based acetate-reducing yeast strain

The results presented above show that, at both high and low acetate-to-glucose ratios, presence of a functional PRK-RuBisCO pathway in an A-ALD-based acetate-reducing *S. cerevisiae* strain impeded *in-vivo* acetate reduction. We recently reported that a 19 amino acid C-terminal extension ('19aa') of the heterologous PRK protein reduced its abundance in engineered yeast strains. This modification was shown to mitigate an overcapacity of the PRK-RuBisCO pathway that led to formation of acetaldehyde and acetate in slow-growing cultures (van Aalst et al. 2023). Such a modification enables adaptation of PRK abundance, while retaining anaerobically inducible transcription of *PRK* (Zitomer and Lowry 1992, Cohen et al. 2001). To investigate whether this modification could also affect interference of the PRK-RuBisCO pathway with the A-ALD-dependent reduction of exogenous acetate, strain IMX2723 (Δ*gpd2* Δ*ald6 eutE* non-ox PPP↑ p*DAN1-PRK*-19aa *cbbM groES/groEL*) was grown in anaerobic batch cultures on 50 g L^{-1} glucose and 50 mmol L^{-1} acetate. In contrast to strain IMX2502, in which the PRK protein did not carry the C-terminal extension, strain IMX2723 consumed all acetate added to the medium (Fig. 3) and did not show a gap in degree-of-reduction balances or reduced biomass yield (Table 4). In addition, it showed a lower glycerol yield than the acetate-reducing strain IMX2503 and, relative to the reference strain IME324, it showed a 6% higher ethanol yield on glucose.

Discussion

Previous studies demonstrated that, in Δ*gpd2* genetic backgrounds, the A-ALD-based acetate-reduction pathway and the PRK-RuBisCO pathway can each efficiently compete for NADH with the remaining glycerol production pathway and, thereby, enable improved ethanol yields in anaerobic *S. cerevisiae* cultures (Papapetridis et al. 2017, 2018). Here, introduction of both pathways in a single *S. cerevisiae* strain was shown to strongly impede *in-vivo* activity of acetate reduction via the A-ALD pathway (Figs 2C and 3C). In addition, anaerobic batch cultures of the dual-pathway strain produced high levels of acetaldehyde (Table 4), a byproduct that was previously found in slow-growing cultures of strains carrying the PRK-RuBisCO pathway (van Aalst et al. 2023).

Acetaldehyde produced by the PRK-RuBisCO pathway might influence *in-vivo* activity of the reversible A-ALD reaction [$\Delta G^{0'}$ = 17.6 kJ mol^{-1} for the reductive reaction (Beber et al. 2022)]. Its reactants NADH/NAD^+ and acetyl-CoA/CoA are conserved moieties, whose concentration ratios are likely to be constrained by their involvement in a large number of metabolic reactions. An estimate of the maximum permissive acetaldehyde concentration for acetyl-CoA reduction ($\Delta G_R^{'} = 0$), based on reported NADH:NAD^+ and acetyl-CoA:CoA ratios in glucose-grown yeast cultures (Additional file 3), yielded a value of 0.35 mmol L^{-1}. Assuming that acetaldehyde diffuses freely out of the yeast cell, the acetaldehyde concentration measured in the fermentation broth was assumed to be the same as the intracellular acetaldehyde concentration. Acetaldehyde concentrations in glucose-acetate grown anaerobic batch cultures of the dual pathway strain IMX2502 were an order of magnitude higher (1.0 to 2.8 mmol L^{-1}, Additional file 1) than this estimated value. In contrast, acetaldehyde concentrations in cultures of the 'single-pathway' acetate-reducing strain IMX2503 did not exceed 0.35 mmol L^{-1} (Additional file 1). This analysis supports the interpretation that the elevated acetaldehyde concentrations in cultures of the dual-pathway strain rendered a net reduction of acetyl-CoA to acetaldehyde by A-ALD thermodynamically impossible.

Acetaldehyde concentrations in anaerobic batch cultures of the dual-pathway strain IMX2502 exceeded those reported for anaerobic batch cultures of congenic 'PRK-RuBisCO-only' strains (van Aalst et al. 2023). This difference may be related to the deletion of *ALD6*, which encodes cytosolic $NADP^+$-dependent acetaldehyde dehydrogenase. *ALD6* was deleted in A-ALD-containing strains, including the dual pathway strain, to prevent a cytosolic ATP-dissipating futile cycle, consisting of A-ALD, Ald6 and the acetyl-CoA synthetase. This futile cycle was implicated in delayed growth of A-ALD-based strains in high-osmolarity media (Papapetridis et al. 2016). In the dual-pathway context, eliminating a key enzyme for acetaldehyde conversion may be less desirable and further research is needed to investigate whether and how expression levels of *ALD6* affect acetaldehyde production by PRK-RuBisCO-based strains.

To simulate the low acetate-to-glucose ratios in first-generation feedstocks for industrial ethanol production, we used a medium containing 50 g L^{-1} glucose and 5 mmol L^{-1} acetate (corresponding to 0.3 g L^{-1} acetic acid). At this low initial concentration of acetate, the biomass-specific rate of acetate conversion by strain IMX2503 (Δ*gpd2* Δ*ald6 eutE*) declined as the acetate concentration decreased (Additional file 3, Supplementary Fig. S1), which indicated a suboptimal affinity of this strain for acetate. While acetate concentrations in industrial media can be 3- to 4-fold higher (Russell 2003, Rasmussen et al. 2015, Phibro Animal Health Corporation 2022), improvement of the kinetics of acetate reduction may be required for fast and complete acetate conversion. This could, for example, be achieved via expression of acetyl-CoA synthetases with better affinity for acetate than the anaerobically expressed isoenzyme Acs2. A candidate protein could be the native Acs1, which is not synthesized under anaerobic conditions and has a 30-fold lower Km than Acs2 [0.32 and 8.8 mmol L^{-1}, respectively (van den Berg et al. 1996)]. However, Acs1 is subject to glucose catabolite inactivation (de Jong-Gubbels et al. 1997), which complicates its application in glucose-grown batch cultures. Alternatively, highly active heterologous acetyl-CoA synthetases, such as an optimized variant of the *Salmonella enterica* enzyme (Shiba et al. 2007, Lian et al. 2014, Zhang et al. 2016) may be applied. Alternatively, strains with improved affinity

for acetate, potentially also due to changes in acetate transport across the plasma membrane, may be obtained by laboratory evolution (Mans et al. 2018). Such experiments could, for example, be based on anaerobic, acetate-limited chemostat cultures of A-ALD-expressing Δ*gpd1* Δ*gpd2* strains (Guadalupe-Medina et al. 2014).

A C-terminal extension of the heterologous PRK was previously shown to reduce acetaldehyde production in slow-growing cultures of PRK-RuBisCO-carrying *S. cerevisiae* (van Aalst et al. 2023). The same strategy for 'tuning' activity of the PRK-RuBisCO pathway enabled complete conversion of acetate in media with low acetate-to-glucose ratios, while maintaining a low glycerol yield and high ethanol yield after acetate depletion. This result provides a first proof-of-principle for efficient conversion of feedstocks for industrial bioethanol production with a low acetate content, thereby preventing continual increase of acetate via recycle water (Ingledew 2003) and improving ethanol yield. Further research should test and further improve this engineering strategy in industrial yeast strains and in concentrated industrial feedstocks. In industrial processes, controlling pathway activity by modification of the abundance of a single enzyme is likely to be a too static approach for application under industrial conditions. Strategies to dynamically regulate expression of the PRK-RuBisCO and A-ALD pathways in response to changes in medium composition could, for example, be based on the design and construction of synthetic regulatory loops based on prokaryotic sensor proteins for acetaldehyde and acetate, such as *Bacillus subtilis* AlsR, which activates transcription in response to acetate (Renna et al. 1993, Frädrich et al. 2012).

Authors' contributions

A.A.: validation, methodology, formal analysis, investigation, writing—original draft, writing—review & editing, and visualization. E.G.: investigation and writing—review & editing. M.J.: writing—review & editing. R.M.: conceptualization, supervision, and writing—review & editing. J.P.: conceptualization, supervision, writing—original draft, and writing—review & editing. All authors read and approved the final manuscript.

Supplementary data

Supplementary data is available at *FEMSYR Journal* online.

Conflict of interest: The Ph.D. project of A.A. is funded by DSM Biobased Products & Services B.V. (Delft, The Netherlands). Royal DSM owns intellectual property rights of technology discussed in this paper.

Funding

This work was supported by the DSM Bio-based Products & Services B.V. (Delft, The Netherlands).

Data availability

Short read DNA sequencing data of the *Saccharomyces cerevisiae* strain IMX2503 were deposited at NCBI under BioProject accession number PRJNA972872. All measurement data used to prepare Figs 1 and 2, Tables 3 and 4 of the manuscript and Figs S1, S2, and S3 of the supplementary materials are available in Additional file 1 and Additional file 2.

References

Andrei M, Munos JW. Inventors; Danisco US Inc, assignee. Altered host cell pathway for improved ethanol production. United States patent US 2017088861A1; 2017 Mar 30.

Argyros A, Sillers W, Barrett T *et al.* Inventors; Lallemand Hungary Liquidity Management, assignee. Methods for the improvement of product yield and production in a microorganism through the addition of alternate electron acceptors. United States patent US 008956851B2. 2015 Feb 17.

Bakker BM, Overkamp KM, van Maris AJ *et al.* Stoichiometry and compartmentation of NADH metabolism in *Saccharomyces cerevisiae*. *FEMS Microbiol Rev* 2001;**25**:15–37.

Beber ME, Gollub MG, Mozaffari D *et al.* eQuilibrator 3.0: a database solution for thermodynamic constant estimation. *Nucleic Acids Res* 2022;**50**:D603–9.

Bertani G. Lysogeny at mid-twentieth century: P1, P2, and other experimental systems. *J Bacteriol* 2004;**186**:595–600.

Blomberg A, Adler L. Physiology of osmotolerance in fungi. *Adv Microb Physiol* 1992;**33**:145–212.

Capaz R, Posada J, Seabra J *et al.* (editors). Life cycle assessment of renewable jet fuel from ethanol: an analysis from consequential and attributional approaches. *Proceedings of the 26th European Biomass Conference and Exhibition*, Copenhagen, Denmark, 2018.

Cohen BD, Sertil O, Abramova NE *et al.* Induction and repression of *DAN1* and the family of anaerobic mannoprotein genes in *Saccharomyces cerevisiae* occurs through a complex array of regulatory sites. *Nucleic Acids Res* 2001;**29**:799–808.

de Bont J, Teunissen A., Inventors; Yeast Company B.V., assignee. Yeast strains engineered to produce ethanol from glycerol. 2012 May 4. International patent WO 2012/067510 A1.

de Jong-Gubbels P, van den Berg MA, Steensma HY *et al.* The *Saccharomyces cerevisiae* acetyl-coenzyme a synthetase encoded by the *ACS1* gene, but not the *ACS2*-encoded enzyme, is subject to glucose catabolite inactivation. *FEMS Microbiol Lett* 1997;**153**:75–81.

Entian K-D, Kötter P. 25 yeast genetic strain and plasmid collections. *Methods Microbiol* 2007;**36**:629–66.

Flikweert MT, de Swaaf M, van Dijken JP *et al.* Growth requirements of pyruvate-decarboxylase-negative *Saccharomyces cerevisiae*. *FEMS Microbiol Lett* 1999;**174**:73–9.

Frädrich C, March A, Fiege K *et al.* The transcription factor AlsR binds and regulates the promoter of the alsSD operon responsible for acetoin formation in *Bacillus subtilis*. *J Bacteriol* 2012;**194**:1100–12.

Froger A, Hall JE. Transformation of plasmid DNA into *E. coli* using the heat shock method. *J Vis Exp* 2007;**6**:e253.

Gietz RD, Woods RA. Genetic transformation of yeast. *BioTechniques* 2001;**30**:816–31.

Guadalupe-Medina V, Almering MJ, van Maris AJ *et al.* Elimination of glycerol production in anaerobic cultures of a *Saccharomyces cerevisiae* strain engineered to use acetic acid as an electron acceptor. *Appl Environ Microb* 2010;**76**:190–5.

Guadalupe-Medina V, Metz B, Oud B *et al.* Evolutionary engineering of a glycerol-3-phosphate dehydrogenase-negative, acetate-reducing *Saccharomyces cerevisiae* strain enables anaerobic growth at high glucose concentrations. *Microb Biotechnol* 2014;**7**:44–53.

Guadalupe-Medina V, Wisselink HW, Luttik MA *et al.* Carbon dioxide fixation by Calvin-Cycle enzymes improves ethanol yield in yeast. *Biotechnol Biofuels* 2013;**6**:1–12.

Ingledew WM. Water reuse in fuel alcohol plants: effect on fermentation. Is a 'zero discharge' concept attainable? In: Jacques K, Lyons T, Kelsall D (eds.), *The Alcohol Textbook*, 4th edn. Nottingham: Nottingham University Press, 2003, 343–54.

Kratzer S, Schüller H-J. Carbon source-dependent regulation of the acetyl-coenzyme a synthetase-encoding gene *ACSI* from *Saccharomyces cerevisiae*. *Gene* 1995;**161**:75–9.

Kumar D, Jansen M, Basu R *et al.* Enhancing ethanol yields in corn dry grind process by reducing glycerol production. *Cereal Chem* 2020;**97**:1026–36.

Kumar D, Singh V. Dry-grind processing using amylase corn and superior yeast to reduce the exogenous enzyme requirements in bioethanol production. *Biotechnol Biofuels* 2016;**9**:1–12.

Lian J, Si T, Nair NU *et al.* Design and construction of acetyl-CoA overproducing *Saccharomyces cerevisiae* strains. *Metab Eng* 2014;**24**:139–49.

Lopes ML, Paulillo SCL, Godoy A *et al.* Ethanol production in Brazil: a bridge between science and industry. *Braz J Microbiol* 2016;**47**:64–76.

Mans R, Daran J-MG, Pronk JT. Under pressure: evolutionary engineering of yeast strains for improved performance in fuels and chemicals production. *Curr Opin Biotechnol* 2018;**50**:47–56.

Mans R, van Rossum HM, Wijsman M *et al.* CRISPR/Cas9: a molecular Swiss army knife for simultaneous introduction of multiple genetic modifications in *Saccharomyces cerevisiae*. *FEMS Yeast Res* 2015;**2**:15.

Mohsenzadeh A, Zamani A, Taherzadeh MJ. Bioethylene production from ethanol: a review and techno-economical evaluation. *ChemBioEng Reviews* 2017;**4**:75–91.

Mooiman C, Bouwknegt J, Dekker WJ *et al.* Critical parameters and procedures for anaerobic cultivation of yeasts in bioreactors and anaerobic chambers. *FEMS Yeast Res* 2021;**21**:foab035.

Mumberg D, Müller R, Funk M. Yeast vectors for the controlled expression of heterologous proteins in different genetic backgrounds. *Gene* 1995;**156**:119–22.

Narendranath NV, Thomas KC, Ingledew WM. Acetic acid and lactic acid inhibition of growth of *Saccharomyces cerevisiae* by different mechanisms. *J Am Soc Brew Chem* 2001;**59**:187–94.

Nijkamp JF, van den Broek M, Datema E *et al.* De novo sequencing, assembly and analysis of the genome of the laboratory strain *Saccharomyces cerevisiae* CEN. PK113-7D, a model for modern industrial biotechnology. *Microb Cell Fact* 2012;**11**:1–17.

Nissen TL, Hamann CW, Kielland-Brandt MC *et al.* Anaerobic and aerobic batch cultivations of *Saccharomyces cerevisiae* mutants impaired in glycerol synthesis. *Yeast* 2000;**16**:463–74.

Nissen TL, Kielland-Brandt MC, Nielsen J *et al.* Optimization of ethanol production in *Saccharomyces cerevisiae* by metabolic engineering of the ammonium assimilation. *Metab Eng* 2000;**2**:69–77.

Papapetridis I, Goudriaan M, Vázquez Vitali M *et al.* Optimizing anaerobic growth rate and fermentation kinetics in *Saccharomyces cerevisiae* strains expressing Calvin-cycle enzymes for improved ethanol yield. *Biotechnol Biofuels* 2018;**11**:1–17.

Papapetridis I, van Dijk M, Dobbe A *et al.* Improving ethanol yield in acetate-reducing *Saccharomyces cerevisiae* by cofactor engineering of 6-phosphogluconate dehydrogenase and deletion of *ALD6*. *Microb Cell Fact* 2016;**15**:1–16.

Papapetridis I, Van Dijk M, Van Maris AJ *et al.* Metabolic engineering strategies for optimizing acetate reduction, ethanol yield and osmotolerance in *Saccharomyces cerevisiae*. *Biotechnol Biofuels* 2017;**10**:1–14.

Pfromm PH, Amanor-Boadu V, Nelson R *et al.* Bio-butanol vs. bio-ethanol: a technical and economic assessment for corn and switchgrass fermented by yeast or *Clostridium acetobutylicum*. *Biomass Bioenergy* 2010;**34**:515–24.

Phibro Animal Health Corporation. 2022. https://fermfacts.com/ferm-facts/yeast-health/ (1 December 2022, date last accessed).

Pronk JT. Auxotrophic yeast strains in fundamental and applied research. *Appl Environ Microb* 2002;**68**:2095–100.

Rasmussen ML, Koziel JA, J-l J *et al.* Reducing bacterial contamination in fuel ethanol fermentations by ozone treatment of uncooked corn mash. *J Agric Food Chem* 2015;**63**:5239–48.

Renewable Fuels Association: Annual Ethanol Production. 2022. https://ethanolrfa.org/markets-and-statistics/annual-ethanol-production (7 January 2022, date last accessed).

Renna M, Najimudin N, Winik L *et al.* Regulation of the *Bacillus subtilis* alsS, alsD, and alsR genes involved in post-exponential-phase production of acetoin. *J Bacteriol* 1993;**175**:3863–75.

Roels J. Simple model for the energetics of growth on substrates with different degrees of reduction. *Biotechnol Bioeng* 1980;**22**:33–53.

Russell I. Understanding yeast fundamentals. In: Jacques K, Lyons T, Kelsall D (eds.), *The Alcohol Textbook*, 4th edn. Nottingham: Nottingham University Press, 2003, 85–120.

Saint-Prix F, Bönquist L, Dequin S. Functional analysis of the *ALD* gene family of *Saccharomyces cerevisiae* during anaerobic growth on glucose: the NADP+-dependent Ald6p and Ald5p isoforms play a major role in acetate formation. *Microbiology* 2004;**150**:2209–20.

Salazar AN, Gorter de Vries AR, van den Broek M *et al.* Nanopore sequencing enables near-complete de novo assembly of *Saccharomyces cerevisiae* reference strain CEN. PK113-7D. *FEMS Yeast Res* 2017;**7**:17.

Secches TO, Santos Viera CF, Pereira TK *et al.* Brazilian industrial yeasts show high fermentative performance in high solids content for corn ethanol process. *Bioresour Bioprocess* 2022;**9**:1–9.

Shiba Y, Paradise EM, Kirby J *et al.* Engineering of the pyruvate dehydrogenase bypass in *Saccharomyces cerevisiae* for high-level production of isoprenoids. *Metab Eng* 2007;**9**:160–8.

Solis-Escalante D, Kuijpers NG, Nadine B *et al.* amdSYM, a new dominant recyclable marker cassette for *Saccharomyces cerevisiae*. *FEMS Yeast Res* 2013;**13**:126–39.

Taherzadeh MJ, Eklund R, Gustafsson L *et al.* Characterization and fermentation of dilute-acid hydrolyzates from wood. *Ind Eng Chem Res* 1997;**36**:4659–65.

Taherzadeh MJ, Niklasson C, Lidén G. Acetic acid—friend or foe in anaerobic batch conversion of glucose to ethanol by *Saccharomyces cerevisiae*? *Chem Eng Sci* 1997;**52**:2653–9.

Thomas K, Hynes S, Ingledew WJA., microbiology e. Influence of medium buffering capacity on inhibition of *Saccharomyces cerevisiae* growth by acetic and lactic acids. *Appl Environ Microb* 2002;**68**:1616–23.

van Aalst AC, de Valk SC, van Gulik WM *et al.* Mans R. Pathway engineering strategies for improved product yield in yeast-based industrial ethanol production. *Synth Syst Biotechnol* 2022;**7**:554–66.

van Aalst AC, Jansen ML, Mans R *et al.* Quantification and mitigation of byproduct formation by low-glycerol-producing *Saccharomyces cerevisiae* strains containing Calvin-cycle enzymes. *Biotechnol Biofuels* 2023;**16**:1–17.

van Aalst AC, Mans R, Pronk JT. An engineered non-oxidative glycolytic bypass based on Calvin-cycle enzymes enables anaerobic co-fermentation of glucose and sorbitol by *Saccharomyces cerevisiae*. *Biotechnol Biofuels* 2022;**15**:1–15.

van den Berg MA, de Jong-Gubbels P, Kortland CJ *et al.* The two acetyl-coenzyme A synthetases of *Saccharomyces cerevisiae* differ with respect to kinetic properties and transcriptional regulation. *J Biol Chem* 1996;**271**:28953–9.

Verduyn C, Postma E, Scheffers WA *et al.* Effect of benzoic acid on metabolic fluxes in yeasts: a continuous-culture study on the regulation of respiration and alcoholic fermentation. *Yeast* 1992;**8**:501–17.

Verduyn C, Postma E, Scheffers WA *et al.* Physiology of *Saccharomyces cerevisiae* in anaerobic glucose-limited chemostat cultures. *Microbiology* 1990;**136**:395–403.

Wei N, Quarterman J, Kim SR *et al.* Enhanced biofuel production through coupled acetic acid and xylose consumption by engineered yeast. *Nat Commun* 2013;**4**:2580.

Zhang GC, Kong II, Wei N *et al.* Optimization of an acetate reduction pathway for producing cellulosic ethanol by engineered yeast. *Biotechol Bioeng* 2016;**113**:2587–96.

Zitomer RS, Lowry CV. Regulation of gene expression by oxygen in *Saccharomyces cerevisiae*. *Microbiol Rev* 1992;**56**:1–11.

Received 22 May 2023; **revised** 24 October 2023; **accepted** 3 November 2023